Radio Science, Volume 31, Number 2, Pages 335–348, March–April 1996

VLF strip holographic imaging of lightning-associated ionospheric disturbances

Jiunn-tsair Chen, Umran S. Inan, and Tim F. Bell

STAR Laboratory, Department of Electrical Engineering, Stanford University, Stanford, California

Abstract. A linear array of very low frequency (VLF) receivers, deployed along a line roughly perpendicular to the direction of signal propagation, enables the determination of the size and location of D region disturbances produced by lightning-induced electron precipitation (LEP) bursts or by lightning-induced heating in the vicinity of the great circle VLF propagation paths. The configuration essentially constitutes a strip hologram so that the width of both the amplitude and phase perturbation of the signal pattern recorded along the strip are simply related to the size and location of the disturbance for the range of altitude profiles of disturbed ionization expected for LEP events. The validity of the approach is demonstrated both analytically for single waveguide-mode propagation and also for a realistic propagation path (Annapolis-Stanford) by using a three-dimensional numerical model of VLF propagation and scattering in the Earth-ionosphere waveguide. We also discuss the criteria by which the spacing of discrete elements along the strip can be optimally choosen.

1. Introduction

Transient and localized disturbances of the D region are now known to occur regularly in association with lightning discharges. The assessment of their geophysical and global significance requires that we determine their spatial distribution (i.e., location and transverse extent). In this paper, we demonstrate the validity of a strip holographic method to "image" lightning-induced ionospheric disturbances and to determine the size and location of the disturbances, without regarding to the altitude profile of density and temperature within the disturbance.

The amplitude and phase of VLF signals propagating in the Earth-ionosphere waveguide are highly sensitive to ionospheric disturbances in the form of electrical conductivity changes resulting from variations in electron density and/or temperature at or below the reflection height (~85 kilometers at night) and within a few hundred kilometers [*Poulsen et at.*, 1993a] of the VLF great circle signal propagation path. Since the relatively low waveguide attenuation at VLF frequencies permits efficient signal detection at distances of many thousands of kilometers, disturbances occurring over a broad region of the ionosphere can be detected. However, the combined effects of the disturbance size, location, electron density and temperature profile are registered as a single VLF signal amplitude and phase variation, making it difficult to extract detailed quantitative information from such measurements at a single site.

To advance further, we need to consider characteristics of the disturbance that can be decoupled and deduced from the measurable quantities. One such characteristic appears to be the transverse size of the disturbance as described below. Based on three dimensional modeling of the scattering of VLF waves from localized disturbances in the Earth ionosphere waveguide, *Poulsen et. al.* [1993b] concluded that the relative amplitude of the VLF signal for different scatter angles is almost independent of the altitude profile of electron density in the perturbed region for the range of profiles expected to occur in lightning-induced ionospheric disturbances. The typical disturbances produced by lightning act primarily as forward scatterers, with a scattering angular width (defined as ~ 15-dB point) of $\pm 7°$ in the forward direction.

Paper number 95RS02079.
0048-6604/96/95RS-02079$08.00

These facts suggest that we can treat the D region disturbance as simply a scatterer with a finite transverse extent. Measurements of the direct signals from a distant VLF transmitter, as well as the signals scattered from the disturbance, at multiple stations appropriately spaced along a line approximately perpendicular to the propagation path, would provide, in principle, a record of the disturbance characteristics that is analogous to a holographic record of an object illuminated by a coherent source. In this paper, we pursue this analogy to show that the combination of the direct plus scattered wave from any D region disturbance can be viewed as a hologram based on which the transverse size of the scattering region can be obtained [*Born and Wolf,* 1965, p. 453]. The analogy with a hologram can most directly be seen for the case of a single waveguide mode signal which scatters from the D region disturbance. As illustrated in Figure 1, the sum of the direct and scattered signals form a hologram pair [*Born and Wolf,* 1965] which in principle could be recorded on a "screen" of antennas across the waveguide. The phase and amplitude of the total signal over the hologram screen could then be used to reconstruct the electrical properties of the D region disturbance. In practice, vertical measurements across this screen are not feasible, but we can still assess the transverse extent of the D region disturbance by measuring the phase and amplitude of the total signal at the bottom strip of our imaginary hologram screen across the waveguide.

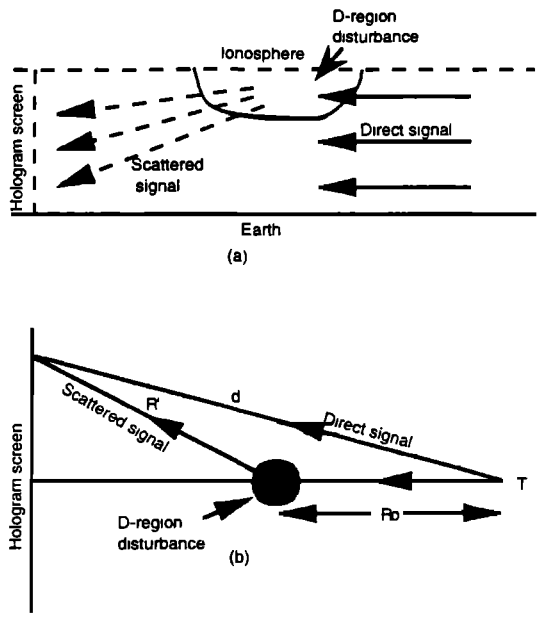

Figure 1. (a) Cross-sectional and (b) top views of the paths of two different (direct and scattered) coherent signals recoded on the hologram screen. Recorded on the bottom line of the hologram screen are the amplitude and phase of the vector sum of these two signals.

In the past decade, a number of aspects of lightning-associated VLF signal amplitude and phase changes, sometimes referred to as "Trimpi" effects, have been investigated [e.g.,*Burgess and Inan,* 1993, *Inan et al.,* 1993, and references therein], including quantitative interpretation of events in terms of precipitated electron fluxes and energies [*Tolstoy et al.,* 1986; *Inan et al.,* 1985; *Inan and Carpenter,* 1987; *Inan et al.,* 1988a], association of events with whistlers [*Inan and Carpenter,* 1986] or with lightning discharges [*Inan et al.,* 1988b], and interpretation of events in terms of different models of VLF signals propagated in the Earth-ionosphere waveguide [*Inan and Carpenter,* 1987; *Dowden and Adams,* 1988, 1989, 1990, 1993; *Poulsen et al.,* 1990, 1993a, b]. Only a few of these works have dealt with the determination of location and size of the D region disturbance, and we briefly discuss these below.

Dowden and Adams [1990] suggested using the phase difference of scattered VLF signals measured at two receiving stations 8.86 kilometers apart to determine the arrival angle of the scattered signal. These authors assumed that the phase difference of the scattered and the unperturbed VLF signals divided by the wave number is the additional distance travelled by the scattered signal. Under that assumption, there exists an ellipse, on which the great circle distances from any point to the transmitter and receiver sum up to be the same as the great circle distance between the transmitter and the receiver plus the additional distance as determined above. Dowden and Adams took the D region disturbance to be at the intersection of this ellipse and the line of signal arrival. There is a problem with this method. Realizing that different points on the ellipse have different scattering angles, this method basically requires that the phase of the scattered VLF signal be independent of scattering angle and disturbance size. However, in general, this is not the case since different points on the ellipse or disturbances of different sizes at the same point on the ellipse can introduce extra phase differences, as is demonstrated in our numerical simulation results discussed later in connection with Figure 8b. For those D region disturbances

at the same location, but having different size, the phase of the scattered VLF signal at the same receiver is quite different, as will be discussed in more detail later. Dowden and Adams also used the group delay, determined from the phase difference at two closely spaced frequencies present in the transmitted signal to calculate the direction of arrival.

Another very crude VLF "imaging" method was utilized by *Inan et al.* [1990], based on the measurement of VLF signals simultaneously at multiple sites. Association of the observed VLF signal perturbations with the D region disturbance was made on the basis of time correlation with prominent radio atmospherics. Simultaneous observations of individual events on subionospheric paths that "cross" one another were used to locate the disturbed ionospheric regions. Absence of perturbations on nearby paths permitted an assessment of the spatial extent of the region with a varying degree of accuracy. This technique provides for very crude spatial resolution and is more suited for the determination of the location of the disturbance than its size.

Instead of using an equal-distance ellipse to determine the location of the disturbance, *Dowden and Adams* [1993] suggested the use of a linear array, introducing the concept of VLF holography (also called "inverse scattering"). Their method was based on a first guess of the axis on which the disturbance is located, and subsequent calculation of the angle of arrival of the signal by pairwise comparison of the phase difference of the VLF signal in order to eliminate a potential 360° phase confusion. The disturbance was taken to be located on the intersection of the axis and the direction of signal arrival. The authors estimated the size of the disturbance assuming that the beam width was inversely proportional to the scattering aperture (although receivers are seldom in the far field zone of the scattered field) and used relatively crude interpolation between the first and the second receivers 550 kilometers apart to determine beam width, and finally determined the disturbance size by comparsion with an analytical model. Thus although the concept of VLF holography was introduced by *Dowden and Adams* [1993], these authors did not relate the width of the amplitude and phase patterns to the disturbance size in the context of a quantitative model. In the present work we further develop the theory of VLF strip holographic imaging. We also demonstrate how the amplitude and phase patterns of the scattered signals can be related to the disturbance size and location using a realistic quantitative model of VLF wave propagation and diffraction in the Earth-ionosphere waveguide.

2. Theoretical Basis

Over the range of typical ground conductivities of interest (10^{-3} to 4 S/m), the propagation of a VLF signal in the Earth-ionosphere waveguide is not sensitively dependent on the ground plane conductivity [*Poulsen et al.*, 1993b]. For simplicity, if we consider a hologram strip perpendicular to the VLF signal propagation path (note that if the strip is not perpendicular to the path, we need to apply some correction factors, as shown in the Appendix), then a symmetry point may be found on the strip, so that the D region disturbance of interest is on the great circle path originating at the transmitter and passing through the symmetry point. The absence of such a symmetry point would mean that the disturbance is outside our region of coverage. According to [*Poulsen et al.*, 1993b], the scattering from typical LEP-induced disturbances is confined to within ±20° of the forward direction (40-dB beam width). In other words, the arrival direction of the scattered signal at a receiver at distances greater than 500 kilometers or so cannot deviate substantially from the direction parallel to the direct signal. For measurable scattered field amplitudes, it is thus likely that a symmetry point of the scattered signal on the hologram strip can be found so that the axis on which the disturbance is located can be determined (Figure 2c). In order to determine the disturbance location along this axis and its size, additional information is needed; the widths of the amplitude and phase pattern as observed on the strip provide this needed information. In the following, we first provide an intuitive discussion of the general case, followed by both graphical and analytical solutions for the simplest case of a single waveguide mode model. In the next section, we then further confirm the utility of the strip holography method by means of the numerical simulation of a realistic propagation path.

Consider Figure 1b. If the D region disturbance forward scatters the incident transmitted signal into a radiation pattern of half-angular width $\alpha << \pi/2$ (for example, where α is defined by the -20-dB point), then the width Δx of this pattern of the screen is just $\Delta x = 2s \tan \alpha$, where s is the distance of the perturbed region from the screen. Clearly, if we know

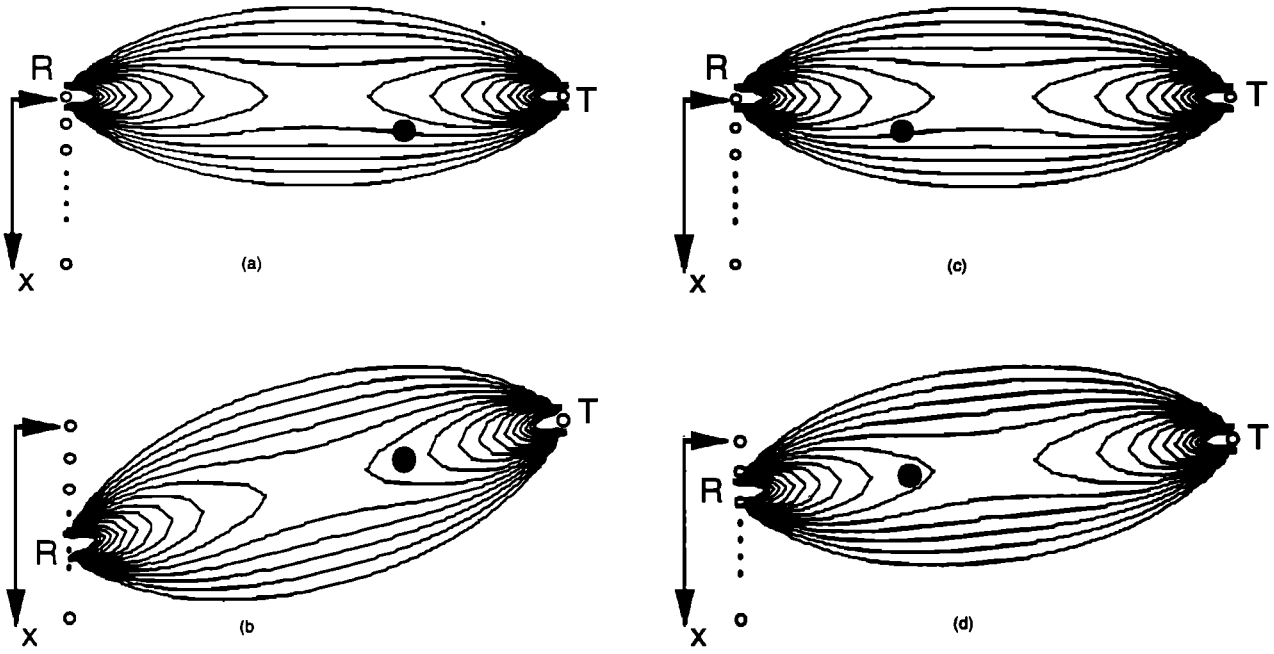

Figure 2. Comparison of the amplitude pattern width of the scattered signal caused by the *D* region disturbance at two different locations. Disturbances infigures 2a and 2b are at the same location, which is closer to the transmitter (T), whereas disturbances in Figures 2c and 2d are also at the same location, which is closer to receiver (R). The solid lines show the equal received scattered power contour lines of the disturbance region which can be rotated to determine the power recieved for receivers at different locations.

α in advance, we can find s merely by measuring Δx along the screen. In practice we do not know α in advance, but we do know that it is related to the horizontal size of the perturbed region [*Poulsen et al.*, 1993b]. Thus intuitively we expect the width of the radiation pattern on the screen to provided information on both the location and horizontal size of the disturbed region.

This conclusion is quite general, since it is not based on any assumptions concerning the mode structure (i.e., single mode or multimode) of the signals propagating in the waveguide, or the electron density and temperature profiles of the *D* region disturbance, or the disturbance size and shape. The reason for this is simply the fact that the angular scattering pattern of typical LEP disturbances is largely invariant to both ionospheric density profile and ground conductivity [*Poulsen et at.*, 1993b]. However, we note that although there appears to be a qualitative relation between the width of the amplitude pattern and the location of disturbance, the absolute value of the scattered signal depends on the perturbation size, electron density and temperature profiles of the disturbed region, the ambient profile, ground conductivity, and the disturbance size, which are all unknown and are likely to vary from event to event. However, since the angular scattering pattern is independent of the electron density and temperature profiles [*Poulsen et al.*, 1993b], the amplitude pattern is also independent of these parameters. Therefore, in our following analysis, we can isolate the two parameters, perturbation location along the axis and the perturbation size, and relate them to the amplitude and phase pattern widths.

To clarify the relationship between the amplitude and phase patterns along the strip and the disturbance location, we now consider a less general case. Shown in Figure 2a are typical simplified equal received scattered-power contours for disturbances of the same size located anywhere between a transmitter T and receiver R. In other words, disturbances located anywhere along any of the contours would scatter the same signal power to the receiver, the outermost contour line representing the locus of lo-

cations which would scatter the lowest power. The contours shown represent only the dominant waveguide mode, so that the received power is proportional to the square of the amplitude received without regard to the signal phase in this simplified case. We assume the amplitude of the angular scattering pattern to be a Gaussian function. In other words, the absolute value of the scattered field is taken to be

$$\frac{1}{\sqrt{\sin\frac{r_1}{R_E}\sin\frac{r_2}{R_E}}}\exp(-k\theta^2)\exp\left[-\mathrm{Im}(S_0)(r_1+r_2)\right]$$

where R_E is the radius of the Earth, r_1 is the distance from transmitting station to the center of the perturbed region, r_2 is the distance from receiving station to the center of the perturbed region, k is a parameter of the Gaussian function mentioned above, θ is scattering angle, and S_0 is the sine of the eigenangle of the dominate mode [*Poulsen et al.*, 1990]. We choose $\mathrm{Im}(S_0)=0.985+2.42\times10^{-2}j$, which corresponds to an ambient ionospheric profile as shown in Figure 6 and a typical ground conductivity of 10^{-3} S/m.

We also note that the contour representation is not precisely correct for disturbance locations within a few wavelengths of either the transmitter or receiver, since a Fraunhofer approximation is implied in the formula given above. Although greatly simplified, the contour representation of Figure 2 is nevertheless quite useful for qualitative analysis. Consider the following two examples in Figure 2, represented by the disturbance regions, as indicated by black spots. For disturbances as located in Figure 2a and 2c, receiver R receives the same power (or amplitude) so that we cannot distinguish between these two disturbance locations by means of measurements only at R. Because of the symmetrical nature of the contour pattern, we can rotate the equal-power pattern to determine the power received at any other location and thus determine the position along the strip at which maximum power would be received, as shown in Figures 2b and 2d. It is clear that the width of the amplitude pattern would be wider for a disturbance region as shown in Figure 2a or 2b, than those shown in Figures 2c or 2d. In general, the amplitude pattern width would be larger for disturbance locations closer to the transmitter. Similar considerations apply for the width of the phase pattern, which can be discussed by constructing equal-phase contours.

3. Analytical Single Waveguide-Mode Solution

Before we undertake quantitative analysis of a realistic case, we introduce an analytical approximation of three dimensional VLF signal propagation in the Earth-ionosphere waveguide to assess the utility of the strip holographic method. For simplicity, we still assume the presence of a single dominant waveguide mode, and consider an ionospheric density disturbance with a cylindrically symmetrical Gaussian shape in the transverse direction. Following the work of *Poulsen et al.* [1990], which is based on earlier work by *Wait* [1964], it can be shown that the ratio of the scattered field e_s to the unperturbed field e_0 is proportional to

$$\frac{e_s}{e_0}\propto\frac{\alpha}{\sqrt{1+j\alpha^2a^2}}\exp\left[-(r_1+jr_2)y_0^2\right]$$

where

$$r_1=\frac{\alpha^4a^2}{1+\alpha^4a^4}$$

$$r_2=\frac{\alpha^2}{1+\alpha^4a^4}$$

$$\alpha=\sqrt{k_0S^0\frac{d}{2x_T(d-x_T)}}$$

and y_0, a, d, and x_T are defined in Figure 3, k_0 is the free space wave vector, and S^0 is the complex sine of the eigenvalue of the local dominant waveguide mode.

In order to apply this formulation to the geometry of our strip hologram, we transform variables to express the ratio of the scattered field e_s to the unperturbed field e_0 in terms of the relevant spatial parameters as shown in Figure 3. We have

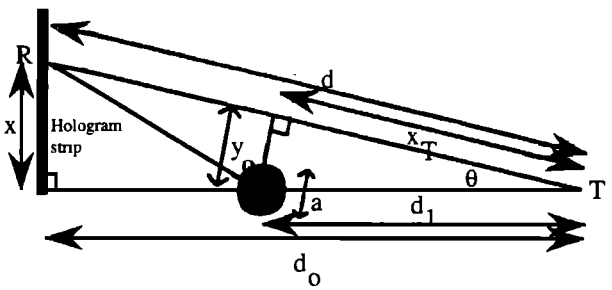

Figure 3. Coordinate system and various parameters used in the analytical formulation of the amplitude and phase pattern widths of the signal received along the hologram strip.

$$\frac{e_s}{e_0} \propto \frac{\alpha}{\sqrt{1+j\alpha^2 a^2}} \exp\left[-(r_1+jr_2)\frac{d_1^2 x^2}{d_0^2+x^2}\right] \quad (1)$$

where

$$r_1 = \frac{\alpha^4 a^2}{1+\alpha^4 a^4}$$

$$r_2 = \frac{\alpha^2}{1+\alpha^4 a^4}$$

$$\alpha = \sqrt{k_0 S^0 \frac{\sqrt{d_0^2+x^2}}{2d_0 d_1(1-\frac{d_0 d_1}{d_0^2+d_1^2})}}$$

and x, a, d_0, d_1, and x_T are defined in Figure 3, and k_0 and S^0 are defined above.

Note from Figure 3 that if we change y_0 or move the disturbance along a line perpendicular to the great circle path between the transmitter (T) and the receiver (R), both the amplitude and the phase of the scattered signal at the receiver would vary in accordance with a Gaussian form. Similarly, we can see from (1) that both the amplitude and the phase of the received signal along the hologram strip are very nearly Gaussian functions, since typically $\alpha^2 a^2 << 1$ and $x << d_0$. Thus we can easily define the symmetry point as the center point of the Gaussian function, define the amplitude pattern width to be the 3-dB (or half amplitude) width, and define the phase pattern width to be the range over which phase varies by $\pm\pi/20$ from that which corresponds to the symmetry point. The value chosen for the phase width range is based on the simulation results discussed below. Also note that the right-hand side of (1) is independent of the electron density and temperature profile of the ionospheric disturbance region, although it does depend weakly on the ambient profile, which influences the complex eigenvalue S^0.

We can now apply (1) to determine the amplitude and phase pattern widths for different disturbance diameters and locations. In (1), the term $\alpha/(1+j\alpha^2 a^2)^{1/2}$ is almost constant for locations along the strip, so that we can neglect it in calculating the amplitude and phase pattern widths. We choose the complex sine of the eigenangle of the dominant mode S^0 to be 0.985 and neglect its imaginary part since it is much smaller (This value for S^0 corresponds to an ambient ionospheric profile shown in Figure 6 and typical ground conductivities of 10^{-3} S/m [*Poulsen et al.*, 1990]). With these assumptions, for a transimitter-receiver strip pair 4000 kilometers apart, we can construct contour patterns representing the locus of points of constant amplitude (3 dB) and phase pattern width ($\pi/20$) as functions of the disturbance size and location with respect to the screen ($d_0 - d_1$) as shown in Figure 4a and 4b. The numbers on the contour lines represent the half widths of the amplitude or phase pattern in kilometers. From Figure 4a, we see that the amplitude pattern width changes with both disturbance location and size. For a disturbance location closer to the transmitter, the amplitude pattern width is wider, as discussed before in connection with Figure 2. It is interesting to note that for $a <\sim 50$ kilometers, the amplitude pattern width increases with decreasing a, whereas for $a >\sim 50$ kilometers, the amplitude pattern width increases with increasing a. For disturbances with very small size ($a \to 0$), there should be isotropic scattering, so that the amplitude would be constant if we assume $d_0 - d_1 >> x$ and the amplitude pattern width would be very large, which is why the amplitude pattern width increases as $a \to 0$. On the other hand, if the disturbance size is very large, and $a\alpha >> 1$, then all points on the screen will be in the near field of the scattering region and the am-

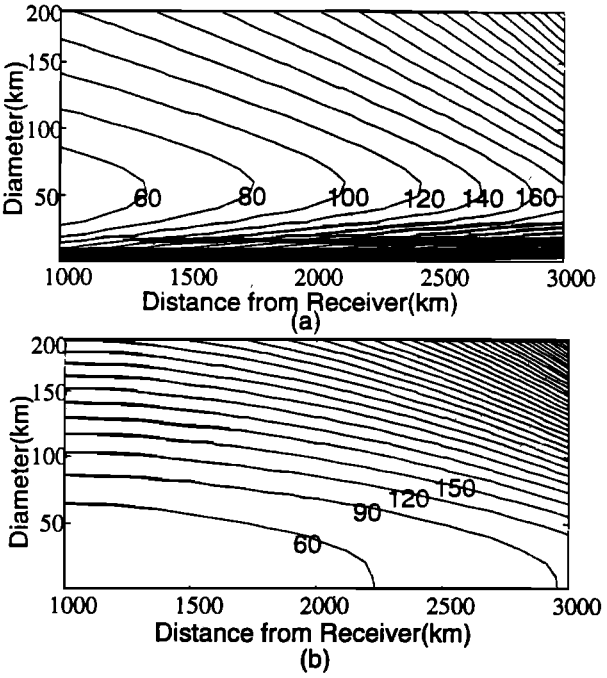

Figure 4. Width of amplitude and phase patterns of the scattered fields divided by the unperturbed fields across the screen as a function of the disturbance location and size.

plitude pattern width will also be very large. As an extreme case, if $a \to \infty$, only forward scatter occurs, all of the beams are parallel to each other and the pattern width is infinite. The behavior of the phase pattern width in Figure 4b is similar to the upper part of Figure 4a. For a disturbance location closer to the transmitter, the phase pattern width is wider, as it also is for larger disturbance sizes. It is clear from the dependences summarized in Figure 4 that if we know both the amplitude and the phase pattern widths from measurements along the hologram strip, we can determine the disturbance location and size. One way this can be achieved graphically is by simply overlapping Figure 4a and Figure 4b and determining the crossing points of contour lines corresponding to the measured pattern widths.

4. A Case Study: NSS-Stanford

We now undertake a case study by numerical solution of the propagation along a realistic great circle path with signal amplitude and phase measured along a holographic strip. For this purpose, we use the three-dimensional multimode VLF propagation code recently developed at Stanford [*Poulsen et al.*, 1993a]. As a representative case, we choose NSS (39° N, 76° W; Annapolis, Maryland, 21.4 kHz) as the transmitter and SU (Stanford University, 37° N, 122° W) to be the first receiver (R1) in our holographic array, which is taken to be perpendicular to the NSS-Stanford path (Figure 5). The path of the VLF signal in this geometry mainly crosses the southern part of the United States, so that the ground plane conductivity is relatively uniform except for mountains on the west side. Using the model, we carry out

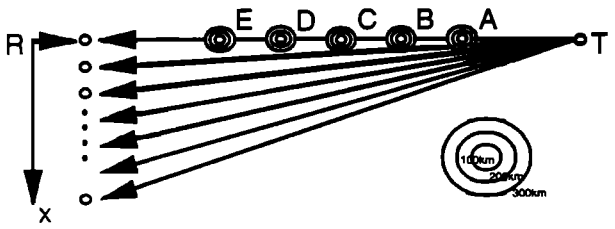

Figure 5. Description of the disturbances of different size and locations used in the numerical simulation. Locations A, B, C, D, and E are on the great circle path between the transmitter (T) and the receiver (R) and are located at fractional distances from the transmitter of 2/8, 3/8, 4/8, 5/8, and 6/8. Three different diameters (100, 200, and 300 kilometers) are considered.

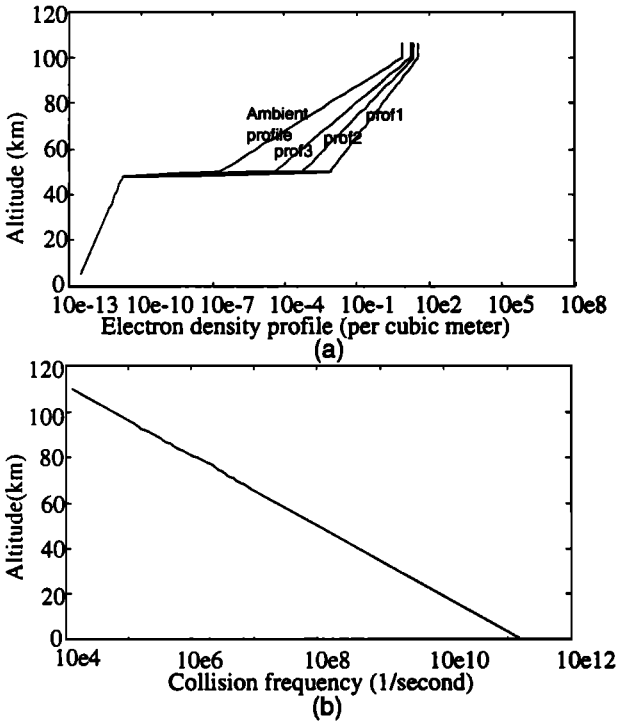

Figure 6. The altitude profile of the electron density and the collision frequency used in this paper. The profiles 1, 2, and 3 span the range of disturbance profiles expected in lightning induced electron precipitation events.

calculations of the amplitude and phase patterns as would be observed along the strip for different disturbance sizes, and locations, as well as electron density and temperature profiles within the disturbance, to assess the circumstances under which information about the disturbance size and location can be inferred from measurements along the strip.

4.1. Dependence on the Disturbance Location

For fixed disturbance size and given disturbance electron density and temperature profiles we investigate the dependence of the received amplitude and phase on the location of ionospheric disturbance along the great circle path (NSS-SU). For this purpose, we consider five different disturbance locations at fractional distances of $2/8, 3/8, 4/8, 5/8, 6/8$, (labeled, respectively, A, B, C, D, and E) from the NSS transmitter, as shown in Figure 5. We assume the lower ionosphere everywhere along the path to be as shown in Figure 6 and the electron density profile within the disturbance to be profile 1, as shown in Figure 6a. The ambient collision frequency profile was taken to

be that in Figure 6b. We obtain results for three different sizes of the disturbance region diameter, namely 100, 200, and 300 kilometers. The numerical results are shown in Figure 7a for the amplitude response and Figure 7b for the phase response along the strip. The quantities plotted are the amplitude and phase of the scattered field as a function of the distance along the strip.

The relation between the amplitude pattern width (or phase pattern width) and the disturbance location are quite apparent from Figures 7a and 7b. Note that the maximum of the scattered field does not change significantly with the disturbance location. Although in principle this behavior might seem to imply that the maximum scattered field amplitude may be used to determine disturbance size, in practice this is not possible since the absolute value of the signal amplitude change varies from event to event, being dependent on many factors such as the lightning intensity, and the precipitation flux level.

Last, we compare the results here with those in Figure 4b. We need to transform the data in Figure 7b (which represents the phase of the scattered field) to express it in terms of the phase of the ratio of the scattered field divided by the unperturbed field in order to directly compare it with Figure 4b, since the unperturbed field is not constant along the holographic strip. Such a transformation results in Figure 7c. Note that in Figure 4b, as the disturbance size a approaches 200 kilometers, the contours are very close to each other, meaning that the phase pattern width increases rapidly with increasing a. A large phase pattern width indicates that the phase itself changes slowly along the holographic strip. Such a behavior is consistent with the results we have in Figure 7c, where phase changes relatively slowly along the strip and almost becomes a horizontal line when the disturbance diameter approaches 200 kilometers or more.

4.2. Dependence on the Disturbance Size

We now consider fixed disturbance locations and electron density and temperature profiles but vary the disturbance size. We choose the same electron density and temperature profiles as shown before in Figure 6, and carry out calculations for three different disturbance diameters, namely 100, 200, and 300 kilometers each for three different disturbance locations A, C, and E (Figure 5). The results of the amplitude and phase responses along the strip are shown respectively in Figures 8a and 8b. Note that the amplitude pattern width does not change significantly but the absolute value of the scattered field is higher for larger disturbances at the same location. Such behavior is entirely expected as a larger disturbance diffracts more power from the direct signal to a receiver position along the strip. As for the almost constant width of the amplitude response, it appears that we can conclude that the amplitude pattern width alone is enough to determine the location of the disturbance for the case in hand. Once we determine the location from the amplitude pattern width, we can use the phase response separately to determine the disturbance size. Note that we do not use the absolute amplitude value to determine the disturbance size since the absolute amplitude of the scattered field nearly proportionally depends on many other parameters (e.g., intensity of lightning, etc.) and varies from event to event. Also note that the phase width in Figure 8b is also proportional to the disturbance size. The larger the disturbance region, the wider the phase width and the slower the phase changes along the strip.

In section 2, we discussed the fact that the assumption made by *Dowden and Adams* [1990], namely that the phase of the scattered field is independent of scattering angle and disturbance size, is generally not true. That this is the case is quite clear from Figure 8b, which shows that for disturbances of different sizes 100, 200, and 300 kilometers, the absolute value of the received phase change at any specific location is quite different (for example, 200 kilometers off the symmetry point on the strip, the phase difference can be over 100°). It thus appears that the phase of the scattered field changes not only due to propagation distance but also due to the disturbance location and size.

4.3. Dependence on the Electron Density and Temperature Profiles

In earlier sections, we assumed that the amplitude and phase pattern widths are independent of the electron density and temperature profiles within the disturbance region and that the physical makeup of the disturbance can be decoupled from location and size. With the numerical model in hand, we are now in a position to quantitatively assess the validity of this assumption. For this purpose, we consider the three different disturbed region electron density profiles shown as profiles 1, 2, and 3, in Figure 6a, and assume a fixed collision frequency profile, as given in Figure 6b. We carry out calcula-

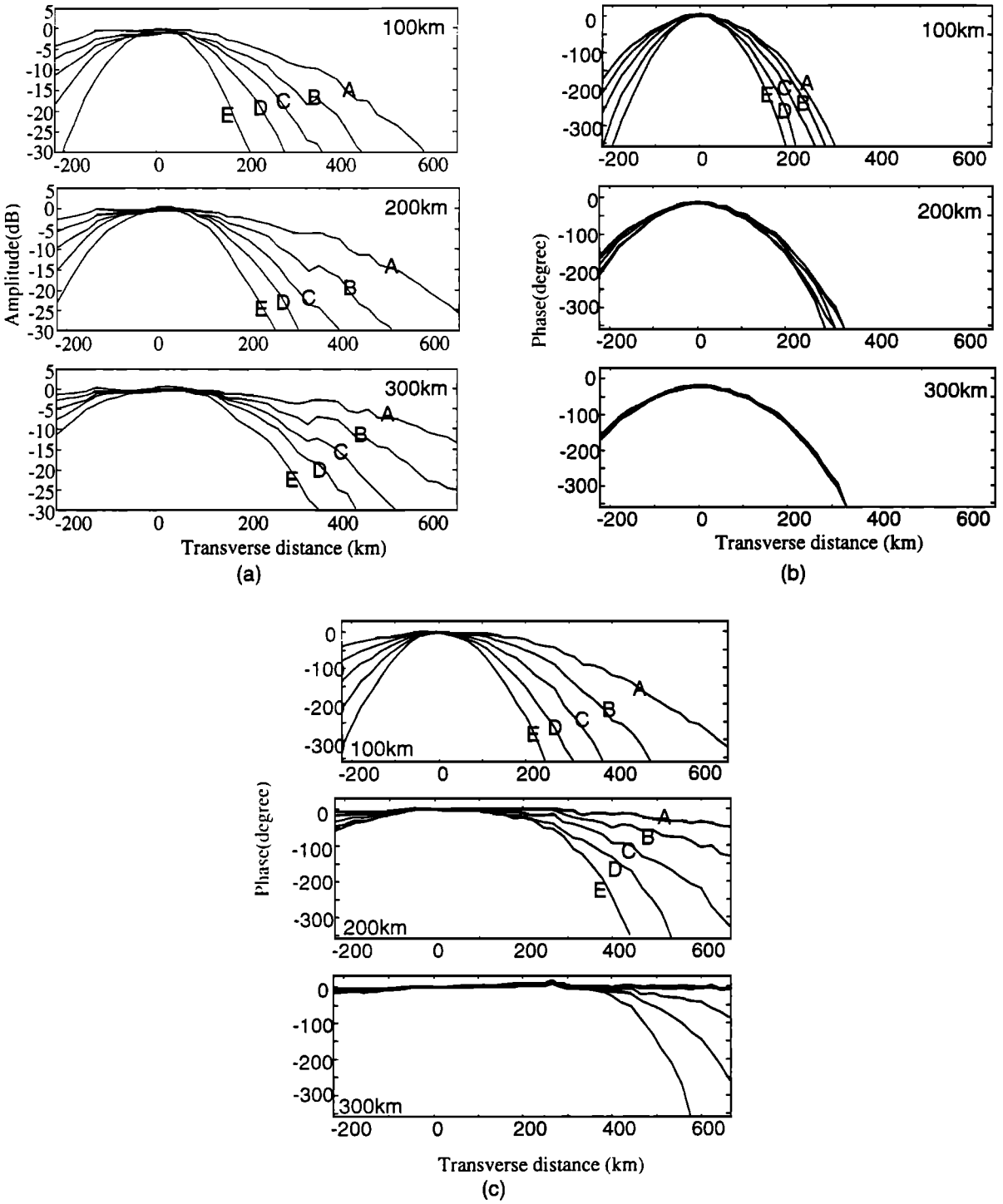

Figure 7. Numerical simulation results of (a) amplitude of the scattered field, (b) phase of the scattered field, and (c) the ratio of the phase of the scattered field versus the unperturbed field as functions of transverse distance along the hologram strip. Results are shown for three different disturbance diameters, 100, 200, and 300 kilometers. A, B, C, D, and E correspond to the five different disturbance locations shown in Figure 5.

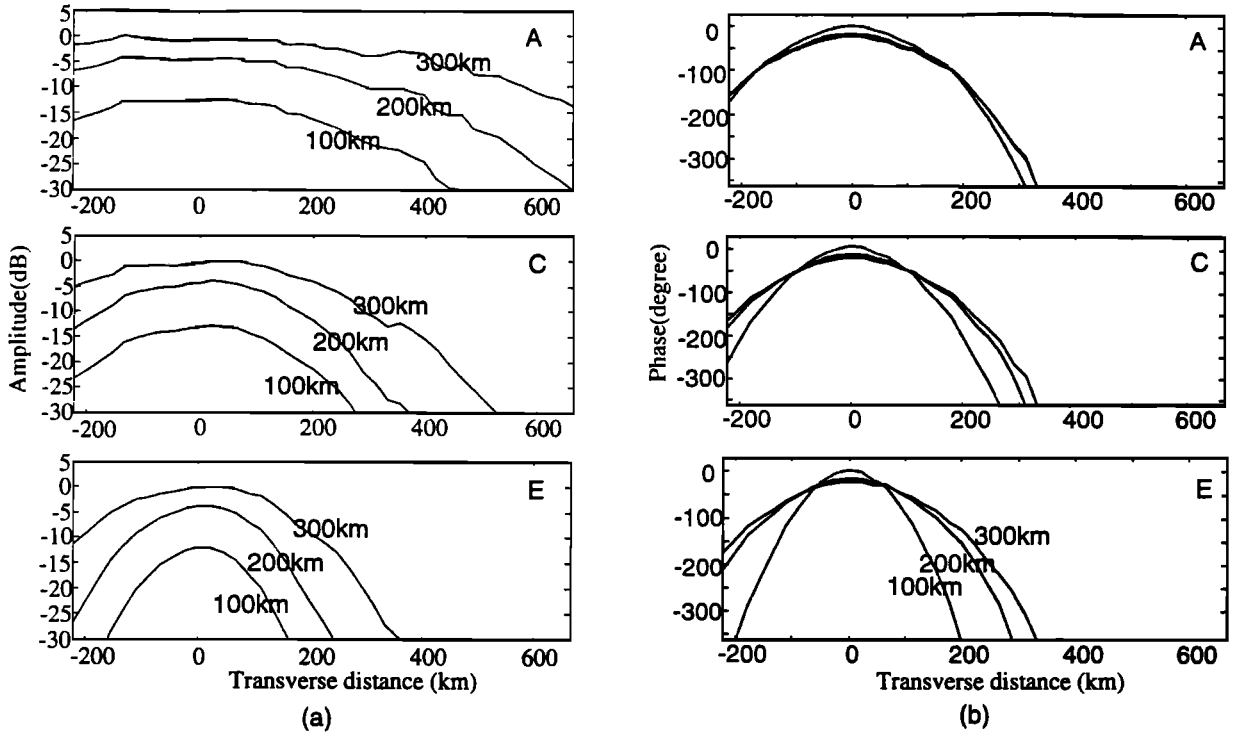

Figure 8. Numerical simulation results of (a) amplitude of the scattered field and (b) phase of the scattered field as functions of transverse distance along the hologram strip. Results for three different locations, A, C, and E (Figure 5), are shown for disturbance diameter of 100, 200, 300 kilometers as indicated.

tions for a fixed disturbance size of 100 kilometers diameter and for disturbance locations A, C, and E as shown in Figure 5. The resulting amplitude and phase pattern are shown respectively in Figures 9a and 9b. According to these, it is apparent that the amplitude pattern widths are essentially independent of the electron density profiles. Disturbances representing larger electron density changes (as, for example, would be expected for LEP bursts with higher peak fluxes), such as profile 1, result in larger scattered field amplitudes, as expected. Furthermore, the phase pattern width also appears to be independent of the electron density profile, confirming our earlier assumptions.

5. Discussion

Our results above indicate that the amplitude and phase patterns as measured along the holographic strip allow us to determine the disturbance location and size, nearly independently of the physical makeup of the disturbance. However, in order to be able to measure the pattern widths, we need to determine the symmetry point (i.e., the point of maximum amplitude) along the strip, which in turn indicates the need to measure the scattered signal along the entire strip. However, in practice, we can only make measurements at discrete points. By analyzing the scattered signal in the spatial frequency domain, we conclude (see below) that receiving sites with 50 kilometers separation would be sufficient to fully recover the signal variation along the strip. If stations are farther apart or if the strip is not long enough, we will have incomplete information. If receivers are too close to each other, we will have redundant information.

In order to determine the required receiver separation, we can apply a spatial Fourier transformation to the complex signal with amplitude and phase as given respectively in Figures 7a and 7b. The results of such a transformation are shown in Figure 10. Note that for disturbances at the same location, the larger the disturbance size, the narrower the spatial bandwidth, as expected. Also note that for a distur-

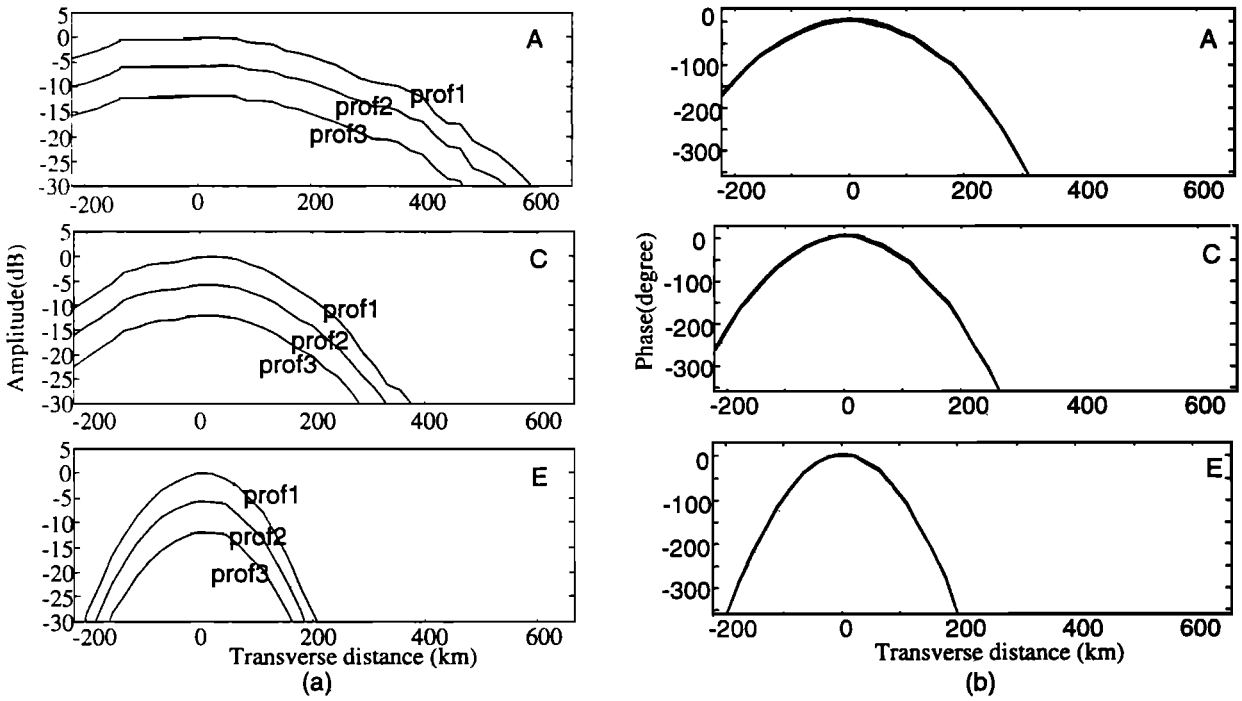

Figure 9. Numerical simulation results of (a) amplitude of the scattered field, and (b) phase of the scattered field as functions of transverse distance along the hologram strip. Results for three different locations, A, C, and E (Figure 5), are shown, for disturbance profiles of 1, 2, and 3 (Figure 6).

bance of the same size, the closer the disturbance to the transmitter, the broader the spatial bandwidth, although the amplitude and phase pattern widths are also larger for those disturbances closer to the transmitters. From Figure 7, we see that the curves labeled D and E are always smoother than those curves labeled A and B, in other words, the amplitude patterns for the D and E cases (which are farther from the transmitter) have a narrower spatial bandwidth. If we consider only the portion of the spectral amplitudes greater than 0.05 times maximum amplitude (which is the minimum measurable scattering signal if we assume the maximum scattering signal is 20-dB weaker than the total VLF signal), a spatial bandwidth of 0.01 km^{-1} appears to be wide enough in most cases, especially when we are interested in those disturbances which are closer to the receiving station. The spatial sampling rate should then be higher than twice the bandwidth, or 0.02 km^{-1}, so that receiving sites should be separated by 50 kilometers or less in order to fully recover the original hologram. From Figure 7a we see that the signal becomes negligibly small at receiving points at distances $\geq$ 400 kilometers from the symmetry point along the strip. Because of symmetry of the amplitude pattern along the strip, we only have to measure signals around the center point and at either side of it. This means that seven or eight stations would be sufficient for holographic imaging of the ionospheric disturbance. However, we need to remember that this is a lower limit, since it only covers those disturbances which occur along a single line (the great circle path from NSS to SU). The longer the holography strip, the broader a region that can be monitored.

If we compare the results of the simplified analytic solution to the numerical modeling results of the previous section, we see some interesting differences. The discrepancies are largely because of the fact that the simplified model only considers a single waveguide mode and neglects the variations of ground conductivity.

In this paper, we have considered only cases of disturbances with circular horizontal cross-section and Gaussian profiles. However, our results can be readily generalized to the case of Gaussian profiles with elliptical cross sections using the results of *Poulsen et*

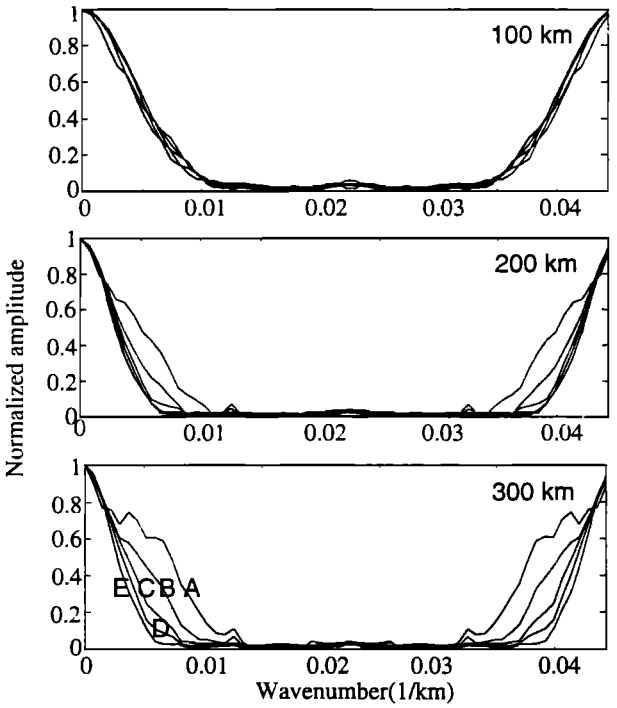

Figure 10. The spatial Fourier transform of the complex signal with amplitude from Figure 7a, and phase from Figure 7b. The amplitude of the spectrum has been normalized to 1 at zero spatial frequency. A, B, C, D, and E represent the five different disturbance locations, as shown in Figure 5. Results are given for three different disturbance diameters, 100, 200, and 300 kilometers, as indicated.

al. [1990, appendix]. Assuming that either the minor or major axis of the ellipse is parallel to the screen, we find that (1), for example, still applies but the parameter a is now interpreted as the width of the ellipse perpendicular to the great circle path between the transmitter and screen. The axis of the ellipse parallel to this great circle path a_1, affects the magnitude of the scattered signal, but not the radiation pattern of the scatterer. Therefore the amplitude and phase pattern shapes along the screen allow the determination of a but not a_1. In general, in order to determine the two dimensional cross section of an arbitrary disturbance, two orthogonal screens would be required. These should be separated and placed in such a way as to monitor a region, such as the midwestern United States, where LEP disturbances are very common.

Our assumption of a Gaussian profile for the disturbances is not critical. The radiation patterns of a few non-Gaussian disturbances are considered by *Poulsen et al* [1993b]. As long as the disturbance is a number of wavelengths in a cross section, the sidelobes of the radiation pattern are generally negligible. Furthermore, the width of the radiation pattern does not depend markedly upon the disturbance profile.

6. Conclusion

In analyzing the inherently complicated problem of VLF signal propagation in the Earth-ionosphere waveguide in the presence of localized disturbances, we have identified two measurable factors: amplitude and phase pattern widths, which are relatively simply related to the ionospheric disturbance size and location but relatively independent of electron density and temperature profiles in the disturbance region. It thus apprears that the amplitude and phase patterns measured along a holographic strip provide one-dimensional boundary conditions for this two-dimensional electromagnetic problem regardless of the third dimension in the vertical direction. This decoupling of otherwise mixed parameters offers promise for direct assessment of the size and location of ionospheric disturbances produced by lightning discharges.

Appendix: Correction for a Nonuniform and Noncollinear Receiver Distribution Along the Hologram Strip

We have shown how a set of receivers deployed along a holographic strip perpendicular to the VLF propagation path can be used to measure the amplitude and phase pattern widths. In this Appendix, we show that the receivers do not have to be deployed along a straight line since corrections can be made to the scattered signal amplitude and phases in order to estimate the pattern width along a strip.

As shown in Figure A1, for any transmitting station T, and for any strip $\overline{AB}$, we can always find a great circle path (GCP) $\overline{GT}$ which connects the transmitter and the strip and which is perpendicular to the strip. In general, the resultant area of coverage may turn out to be very small, although we do not have to make any corrections for receivers not being along the same line. The following procedure would allow the least amount of estimation and also provide max-

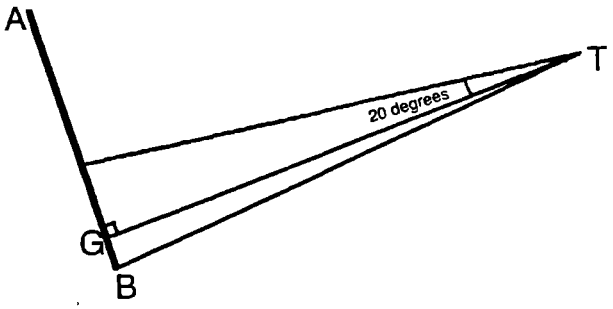

Figure A1. For any strip we can always find a GCP from transmitter T to the strip which is perpendicular to the strip.

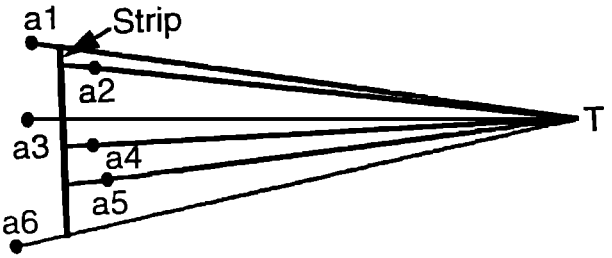

Figure A2. Steps (1),(2) of procedure to estimate an approximate strip.

imum coverage: (1). Draw a GCP from T to each element antenna, as shown in Figure A2. (2) Find a strip which is perpendicular to all the GCPs and which minimizes $|a_1| + |a_2| + |a_3| + \cdots$. (3) Estimate the signal received on the strip to be $e_s \cdot \exp(\pm jka_i)$ where e_s is the scattered field received on element antenna i and the plus corresponds to the situation when the distance from the transmitter to the location along the strip is shorter than that to the antenna element. (Note that the different waveguide modes all travel roughly at the same speed of light, so that over short distances such as a_i, the phasors of different modes would maintain the same relationship with respect to one another.) (4) Assuming that the length of the strip is l, the number of antenna elements is n, and that x respresents the distance along the strip, substitute the signals received at n stations on the strip corresponding to n different nonequally spaced x values into the following equation:

$$e_s(x) = \sum_{i=-\infty}^{\infty} A_i \cdot \operatorname{sinc}\left[\frac{n-1}{l}x - i\right] \qquad \text{(A1)}$$

where A_i is the signal received at n equally spaced antenna along the strip. This procedure leads to n equations in terms of n unknowns A_i. After solving for A_i, (A1) provides an estimate of the signal as it would have been measured on the strip. (If the signal to noise ratio S/N is high enough, we can perfectly recover the signal on the strip. If receiving stations are far from equally spaced, we need S/N to be even higher to recover the original signal on the strip.)

Note that the extra distances we calculated above are those of the unperturbed waves, not those of the scattered waves. The extra distances that the scattered waves travelled should be calculated from the scattering center. Although the location of the D region disturbance is not known, the directions of the unperturbed wave and the scattered wave are almost parallel (less than $\pm 20°$), and the extra distances are much smaller than the total distance that the scattered wave travels. Thus we can use the extra distances calculated from the transmitter to approximately estimate those from the scattering center. For this, we can start with an approximate scattering center location and after several iterations, the result will converge to the correct location of the D region disturbance.

Acknowledgments. This research was sponsered by Office of Naval Research (ONR) grant N00014-94-1-0100 at Stanford University.

References

Born, M., and E. Wolf, *Principles of Optics*, Pergamon, New York, 1965.

Burgess W. C., and U. S. Inan, The role of ducted whistlers in the precipitation loss and equilibrium flux of radiation belt electrons, *J. Geophys, Res., 98,* 15,643-15,665, 1993.

Dowden, R. L., and C. D. D. Adams, Phase and amplitude perturbations on subionospheric signals explained in terms of echoes from lightning-induced electron precipitation ionization patches, *J. Geophys. Res., 93,* 11,543-11,550, 1988.

Dowden, R. L., and C. D. D. Adams, Phase and amplitude perturbations on the NWC signal at Dunedin from lightning-induced electron precipitation, *J. Geophys. Res., 94,* 497-503, 1989.

Dowden, R. L., and C. D. D. Adams, Location of lightning-induced electron precipitation from measurement of VLF phase and amplitude perturbations on spaced antennas and on two frequencies, *J. Geophys. Res., 95,* 4135-4145, 1990.

Dowden, R. L., and C. D. D. Adams, Size and location of lightning-induced enhancements from measurement of VLF phase and amplitude perturbations on multiple antennas, *J. Atmos. Terr. Phys., 55(10),* pp 1335-1359, 1993.

Inan, U. S. and D. L. Carpenter, On the correlation of whistlers and associated subionospheric VLF/LF perturbations, *J. Geophys. Res., 91,* 3106-3116, 1986.

Inan, U. S. and D. L. Carpenter, Lightning-induced electron precipitation events observed at L = 2.4 as phase and amplitude perturbations on subionospheric VLF signals, *J. Geophys. Res.*, *92*, 3293-3303, 1987.

Inan, U. S., D. L. Carpenter, R. A. Helliwell, and J. P. Katsufrakis, Sub-ionospheric VLF/LF phase perturbations produced by lightning-whistler induced particle precipitation, *J. Geophys. Res.*, *90*, 7457-7469, 1985.

Inan, U. S., W. C. Burgess, T. G. Wolf, D. C. Shafer, and R. E. Orville, Lightning-associated precipitation of MeV electrons from the inner radiation belt, *Geophys. Res. Lett.*, *15*, 172-175, 1988a.

Inan, U. S., D. C. Shafer, W. Y. Yip, and R. E. Orville, Subionospheric VLF signatures of nighttime *D* region perturbations in the vicinity of lightning discharges, *J. Geophys. Res.*, *93*, 11,455-11,472, 1988b.

Inan, U. S., F. A. Knifsend, and J. Oh, Subionospheric VLF "imaging" of lightning-induced electron precipitation from the magnetosphere, *J. Geophys. Res.*, *95*, 17,217-17,231, 1990.

Inan, U. S., J. V. Rodriguez, and V. P. Idone, VLF signatures of lightning-induced heating and ionization of the nighttime *D* region, *Geophys. Res. Lett.*, *20*, 2355-2358, 1993.

Poulsen, W. L., T. F. Bell, and U. S Inan, Three-dimensional modeling of subionospheric VLF propagation in the presence of localized D region perturbations associated with lightning, *J. Geophys. Res.*, *95*, 2355-2366, 1990.

Poulsen, W. L., U. S Inan, and T. F. Bell A multiple-mode three dimensional model of VLF propagation in the Earth-ionosphere waveguide in the presence of localized D region disturbances, *J. Geophys. res.*, *98 No. A2.* 1705-1717, 1993a.

Poulsen, W. L., T. F. Bell, and U. S Inan, The scattering of VLF waves by localized ionospheric disturbances produced by lightning-induced electron precipitation, *J. Geophys. Res.*, *98*, 15,553-15,559, 1993b.

Tolstoy, A., T. J. Rosenberg, U. S. Inan, and D. L. Carpenter, Model predictions of subionospheric VLF signal perturbations resulting from localized electron precipitation-induced ionization enhancement regions, *J. Geophys. Res.*, *91*, 13,473-13,482, 1986.

Wait, J. R., Influence of a circular ionospheric depression on VLF porpagaton, *Radio Sci.*,, *68D*, 907-914, 1964.

Tim F. Bell, Jiunn-tsair Chen and Umran S. Inan, STAR Laboratory, Department of Electrical Engineering, Stanford University, Durand 324, Stanford, CA 94305-4055.

(Received March 20, 1995; revised July 3, 1995;
accepted July 7, 1995.)